Journal of Toxicology and Environmental Health Sciences Vol. 3(10), pp. 286-297, 14 September, 2011
Available online at http://www.academicjournals.org/JTEHS
ISSN 2006-9820 ©2011 Academic Journals

Full Length Research Paper

Adsorption of Rhodamine B dye from aqueous solution onto acid activated mango (*Magnifera indica*) leaf powder: Equilibrium, kinetic and thermodynamic studies

Tabrez A. KHAN, Sangeeta SHARMA and Imran ALI*

Department of Chemistry, Jamia Millia Islamia, Jamia Nagar, New Delhi-110025, India.

Accepted 3 August, 2011

Acid activated mango leaf powder (MLP) was employed for removal of the rhodamine B (RB) dye from aqueous solution. Batch adsorption studies were carried out under varying conditions of dye concentration, adsorbent dose, particle size, contact time, pH, and temperature. Removal efficiency was 77% in 45 min with 6.0 pH, 25 g/L as dose, 250 mg/L RB concentration and 30°C temperature. The equilibrium data the best fitted with Langmuir model. The adsorption followed Lagergren pseudo-first order kinetics. The values of free energy change (Δ*G*°), enthalpy change (Δ*H*°), and entropy change (Δ*S*°) indicated the process to be spontaneous. The diffusion studies indicated that adsorption initially takes place by external mass transfer and later by intraparticle diffusion. The results indicate that MLP is a good adsorbent for the removal of RB from wastewater.

Key words: Acid activated mango leaf powder, adsorption, Rhodamine B, isotherms, kinetics, thermodynamics.

INTRODUCTION

Many industries such as textile, paper, rubber, plastics, paints, printing, and leather discharge colored effluents indiscriminately, which cause pollution in receiving water bodies. The problem is more severe for textile industries because they are major consumers of the dyes, most of which are toxic and non-biodegradable. The huge volume of generated wastewater, when released into the environment, causes adverse effects on aquatic ecosystem and human life. The colored water is not only aesthetically objectionable but depletes sunlight penetration which reduces the photosynthetic activity in aquatic plants impeding their growth. Many dyes may cause allergic dermatitis, skin irritation, dysfunction of kidney, liver, brain, reproductive and central nervous system. Besides, some are suspected carcinogens and mutagens.

Rhodamine B (RB) is used mostly in paper printing, textile dyeing, and leather industries. It is carcinogenic, and may cause irritation, redness and pain in eyes and skin. When inhaled, it causes irritation in respiratory tract with symptoms of coughing, sore throat, labored breathing and chest pain. If swallowed, RB is likely to cause irritation to the gastrointestinal tract. Therefore, it is imperative that proper treatment of the dye effluents for color removal is carried out before its discharge.

Numerous methods exist for the treatment of textile wastewater with varying degree of success (Mondal, 2008; Khan et al., 2009; Gupta et al., 2003, 2005). Amongst these, the adsorption technique using low cost adsorbents derived from various natural, agricultural, and industrial wastes (Crini, 2006; Allen and Koumanova, 2005; Ali, 2010) is most widely employed in wastewater treatment. The activated carbon is most commonly used adsorbent. In recent years the activated carbon prepared from agricultural wastes has attracted considerable attention for decolorization of dye wastewater (Amin, 2008; Tan et al., 2007; Preethi et al., 2006) mainly because of its large surface area and high porosity. A number of studies using activated carbon from different agricultural waste materials, which include Kapok hull (Tan et al., 2007), Rice husk (Preethi et al., 2006), Banana bark (Arivoli et al., 2009), *Thespusia populinia*

*Corresponding author. E-mail: drimran_ali@yahoo.com.

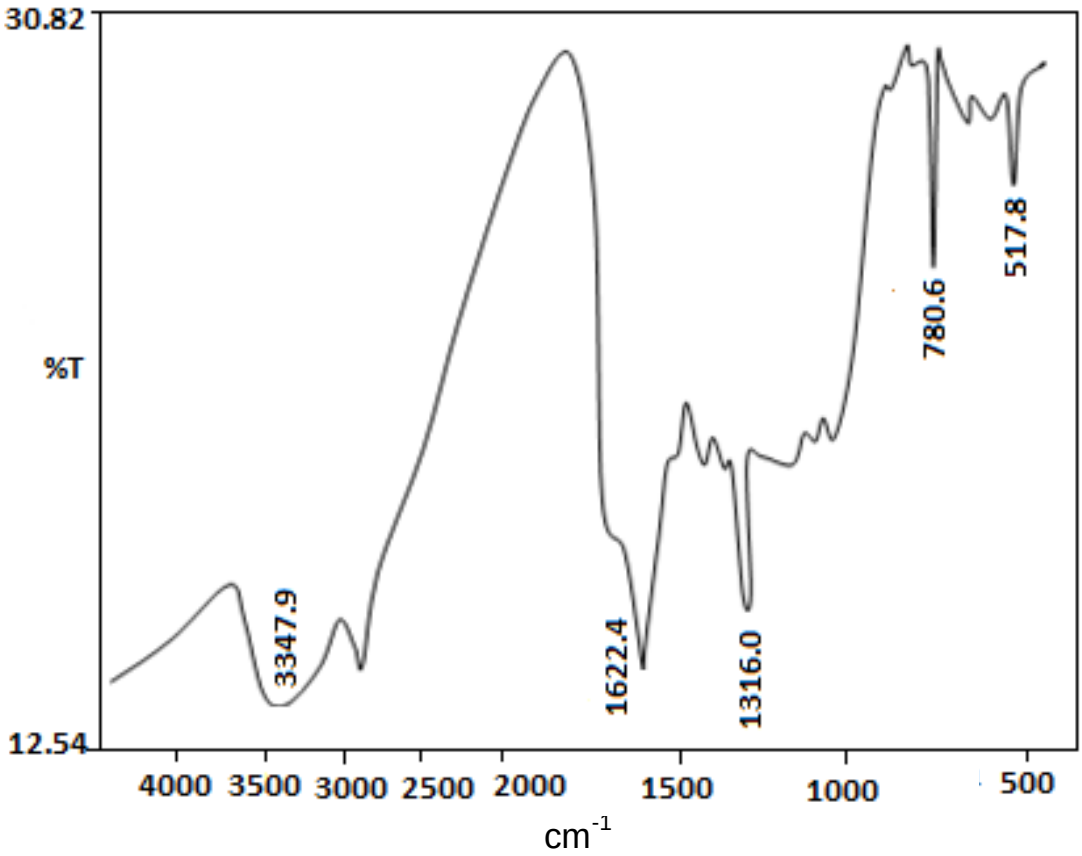

Figure 1. FTIR spectra of MLP.

bark (Hema and Arivoli, 2009), Pandanus leaves (Hema and Arivoli, 2007), Phoenix Sylvestric leaves (Arivoli and Thenkuzhali, 2008), cassava peels (Sivaraj et al., 2001), and Jackfruit peel (Inbaraj and Sulochana, 2006) have been reported for RB removal from aqueous solution. In this study, activated carbon of mango leaves has been evaluated as a low cost adsorbent for the removal of RB from aqueous solution.

MATERIALS AND METHODS

All chemicals used were of analytical grade and used without further purification. The surface textures of mango leaf powder (MLP) before and after adsorption were observed by Scanning electron microscope (JEOL, model 3300). The Fourier Transform Infrared (FT-IR) spectrum [3500 to 500 cm^{-1} (Figure 1)] was recorded by Perkin Elmer 3λ spectrometer. pH measurements were done with a pH meter (model APX 175 E/C, Elico, India).

Preparation of acid activated mango leaf powder (MLP)

Mango leaves were collected from the local areas of the Faridabad District, Haryana, India. The leaves were washed with water and dried at 70 to 80°C in an oven. The dried leaves were crushed into powder, and boiled in distilled water for 3 to 4 h to remove the color. It was filtered and the residue was soaked in dilute H_2SO_4 for about 2 h. The residue was dried at 110°C for 8 h, grounded and finally sieved to different particle sizes (<75, 75-125, 125-150, 150-180, 180-250 and 250-300 µm) and stored in air tight containers.

Preparation of dye solutions

The dye solutions of appropriate concentration (1 to 500 mg/L) were prepared by diluting the stock solution (1000 mg/L) with distilled water. The pH adjustment was carried out using 0.1 N HCl or NaOH solutions.

Batch adsorption studies

The equilibrium adsorption of Rhodamine B dye onto MLP was carried out in triplicate by shaking 0.5 g of MLP with 50 ml of various concentrations (C_i = 5, 10,…….300 mg/L), solution for different time intervals at 30°C in a water bath-cum-mechanical shaker. An approximately 10 ml portion of the solution was withdrawn after the desired time interval and then centrifuged. The equilibrium concentration (C_e) of the dye in supernatant liquid was determined spectrometrically at a λ_{max}= 555 nm. For adsorption isotherm studies, 25 g/L of adsorbent with 50 ml of different concentrations of the dye solution (5 to 300 mg/L) were shaken at their equilibrium contact time (45 min) at 20 to 30°C at pH 7. The adsorption kinetic studies were performed using 25 g/L of MLP and the dye concentration in solution as 250 mg/L, at pH 7. The solution was shaken at different time intervals in the temperature range 20 to 30°C. The residual concentration of the dye which was not

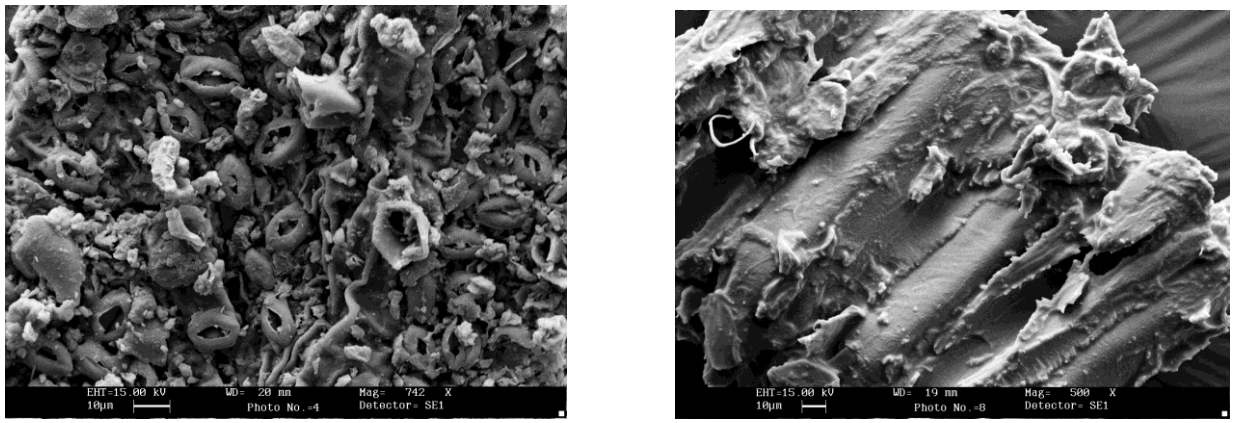

a b

Figure 2. SEM micrographs of MLP before (a) and after adsorption (b).

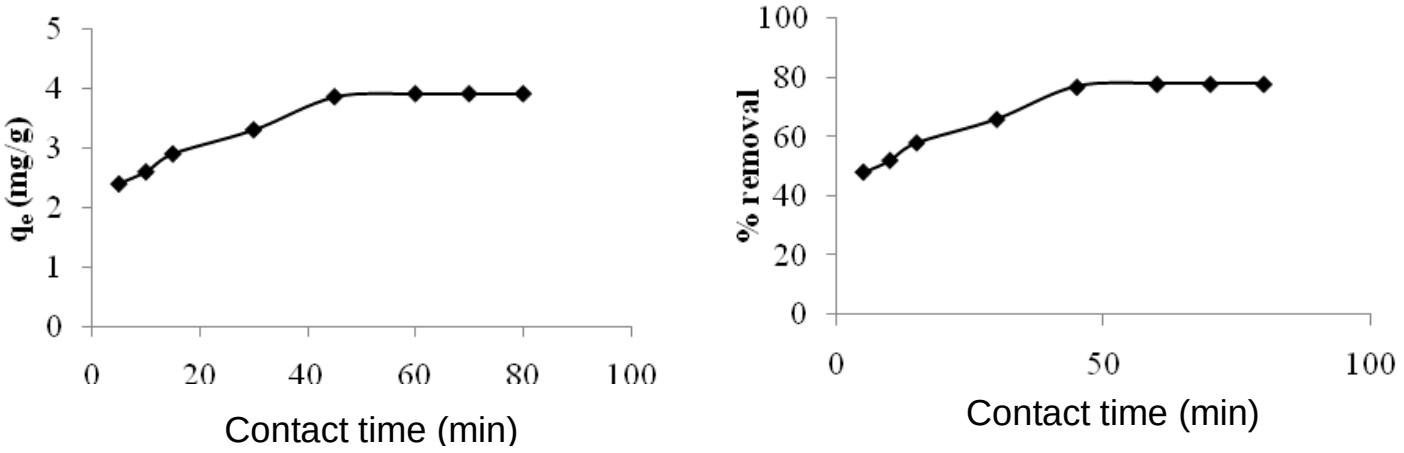

Figure 3. Effect of contact time on adsorption of Rhodamine B.

adsorbed was determined spectrometrically.

RESULTS AND DISCUSSION

Characterization of the adsorbent

FTIR spectrum of MLP (Figure 1) exhibited various peaks at 3347.9 cm^{-1} (N-H), 2900.0 cm^{-1} (C-H stretching), 1622.4 cm^{-1} (C=C or C=N stretching vibrations), 1316.0 cm^{-1} (C-O stretch of primary alcohol), 1050.0 cm^{-1} (C-O stretching of keto ether), 900.0 cm^{-1} (C-H deformation out of plane), and 780.6 cm^{-1} (C-H stretching in aromatic ring) respectively. It is clear from these peaks that the adsorbent has many functional groups. Most probably these functional groups form hydrogen bondings with adsorbate, which are responsible for adsorption.

SEM micrograph of MLP (Figure 2) shows that the adsorbents surface irregular, rough and highly porous, indicating the possibility of its good adsorption properties.

In the SEM image of RB absorbed MLP, the layer of adsorbed dye are clearly visible.

Effect of contact time

The adsorption experiment was carried out with 50 mg/L RB solution, 10 g/L MLP for 5 to 80 min at pH 6.0. The results are depicted in Figure 3. It shows that rate of RB uptake was rapid in the initial 5-30 min. (q_e; 2.4-3.3 mg/g), which became slower during 30 to 45 min (q_e; 3.3-3.85 mg/g) and attaining equilibrium in 45 min. The percent removal followed the same pattern and increases from 48 to 77% when time increased from 5 to 45 min. This is expected because a large number of surface sites are available for adsorption at the initial stages and after a lapse of time, the remaining surface sites are difficult to occupy because of repulsion between RB molecules of

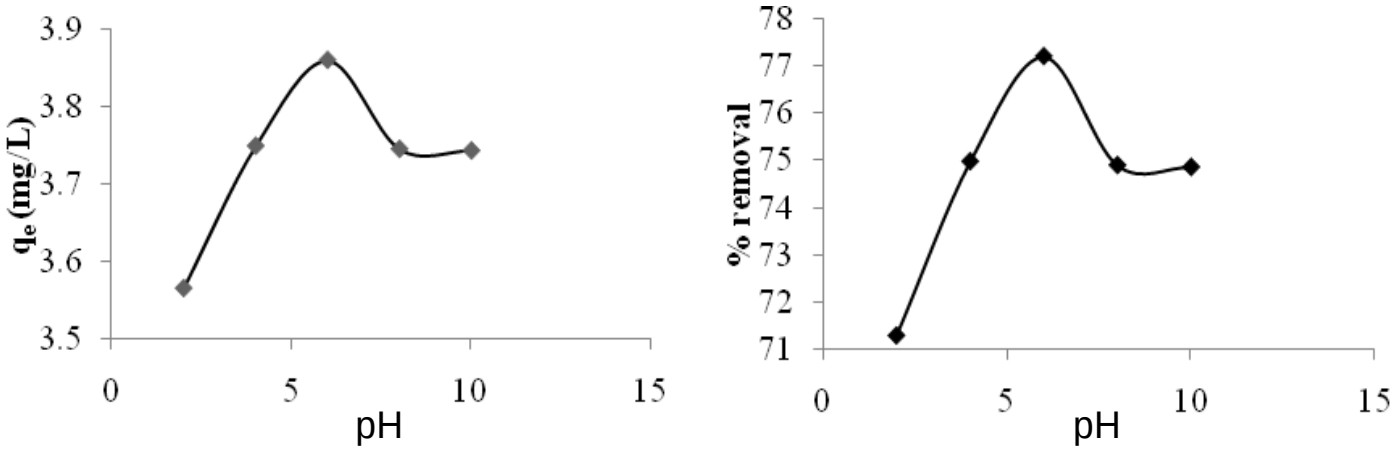

Figure 4. Effect of pH on removal of Rhodamine B.

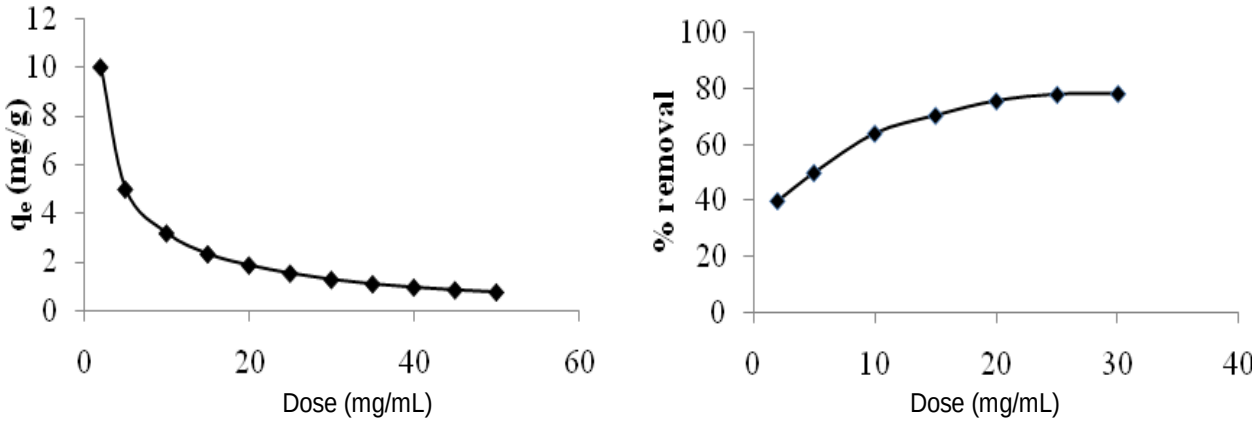

Figure 5. Effect of adsorbent dose on adsorption of Rhodamine B.

the solid and bulk phases (Poots et al., 1976).

Effect of pH

Effect of pH on the adsorption capacity of MLP was studied in the pH range 2 to 10, with 50 mg/L dye solution, adsorbent dose 10 g/L at room temperature (Figure 4). The q_e values initially increased from 3.565 to 3.86 mg/g (71.3 to 77.2%) with increase in pH, with optimal uptake at pH 6. The RB uptake, however, decreased from 3.86 to 3.743 mg/g (77.2 to 74.86%) in the pH range of 6 to 8. Similar trend in q_e values was observed by other workers for basic dye (Low et al., 1995; Rajamohan, 2009). This trend may be explained on the basis of the fact that at pH below 6, the RB ions readily enter into the pore structure of the MLP surface, whereas at pH beyond 6, the zwitterionic form of RB in water aggregated to form a dimer, which was unable to enter into the pores (Ramuthai et al., 2009).

Effect of MLP dose

The effect of varying MLP amount (2 to 30 g/L) on the adsorption capacity of RB (50 mg/L) is shown in Figure 5. The adsorption capacity decreased from 10 to 1.303 mg/g, with increase in the adsorbent amount but the percent adsorption increased from 40 to 77%. The enhanced percent adsorption of RB may be due to the increased surface area and available adsorption sites with increase in MLP dose. The maximum dye uptake occurred at 25 g/L dose, hence, it was chosen as the optimized dose.

Effect of particle size

The amount of dye sorbed with varying particle sizes of MLP (<75, 75-125, 125-150, 150-180, 180-250 and 250-300 µm) increased with decreasing particle size (Figure 6). The percentage of removal decreased from 78.1 to

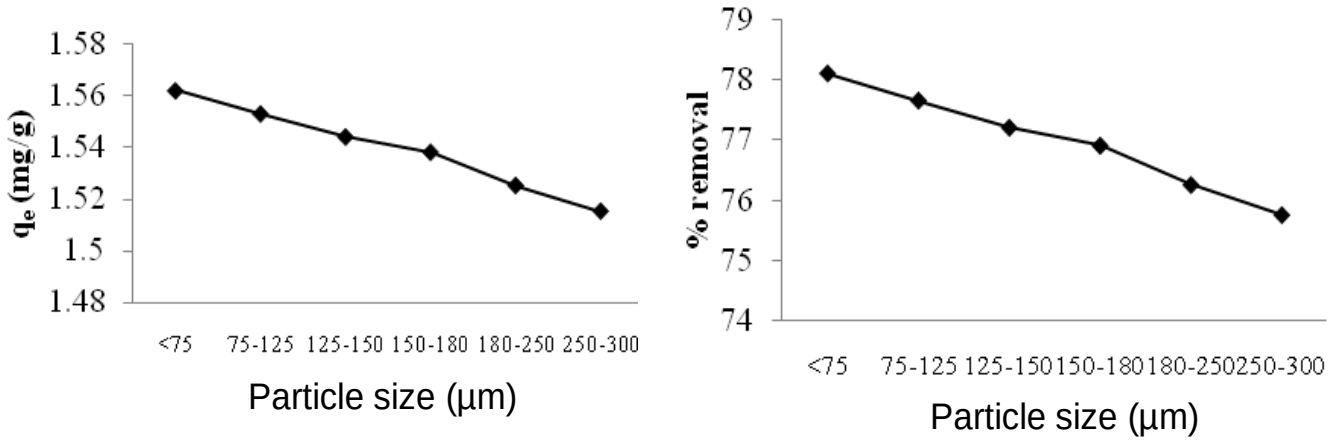

Figure 6. Effect of particle size on adsorption of Rhodamine B.

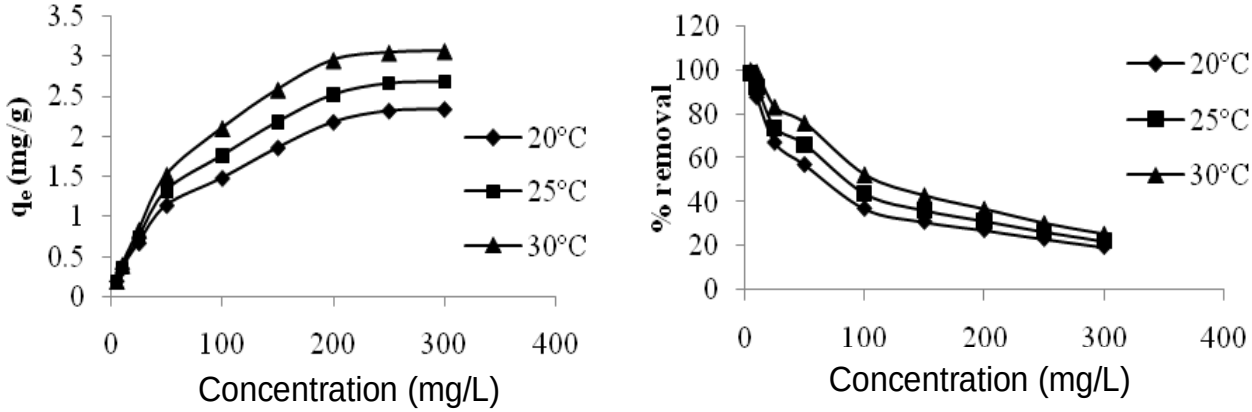

Figure 7. Effect of temperature on adsorption of Rhodamine B.

70% when particle size increases from >75 to 250-300 µm. This could be attributed to increased surface area of the smaller particles. Although the maximum adsorption was observed for <75 µm size, we have chosen 150 to180 µm (with maximum 77% removal) as the optimum particle size mainly due to the reason that it may be conveniently used in the column studies.

Effect of Initial concentrations and temperature

The effect of initial dye concentration of RB (5 to 300 mg/L) on adsorption was studied at the optimized conditions at three different temperatures (20 to 30°C). It was observed (Figure 7) that with increase in the initial RB concentration the percentage removal decreased from 99.8 to 25.5, 99 to 22.34, and 98 to 19.5, while the actual amount of RB sorbed per unit mass of MLP increased from 0.199 to 3.06, 0.198 to 2.68 and 0.196 to 2.34 mg/g at 30, 25 and 20°C, respectively. The maximum dye uptake took place at 250 mg/L RB concentration. The percentage removal decreased because at higher concentration the available sites on the adsorbent become limited. However, adsorption capacity increased as dye concentration increased, it might be due to the increase adsorption rate and utilization of all available adsorption sites at higher concentration. As shown in Figure 7, the percent removal and the amount of RB sorbed increased when the temperature is increased, indicating an endothermic adsorption process. The favored adsorption at higher temperature may be ascribed to either increase in the available adsorption sites, or rise in the diffusion of RB.

Adsorption isotherms

The adsorption isotherms are important to describe the sorbate-adsorbent interaction. The isotherm data were analyzed by fitting them into Langmuir, Freundlich, Dubinin-Radushkevich, and Temkin isotherm models to find out the suitable model that may be used for design

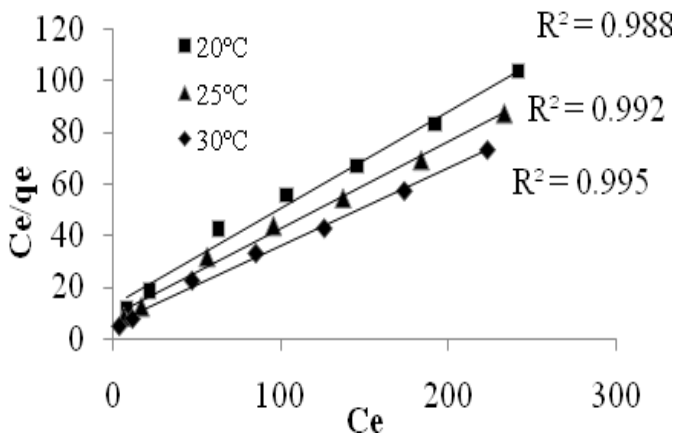

Figure 8. Langmuir isotherm plot.

Table 1. Isotherm constants and regression data for various adsorption isotherms.

Isotherm model	20°C	25°C	30°C
Langmuir			
Q_m	2.67	2.98	3.31
b	12.96	5.51	8.965
R_L	0.000309	0.000725	0.000446
R^2	0.988	0.995	0.992
Freundlich			
K_f	0.3334	0.5970	0.4295
n	2.7247	3.125	2.8490
R^2	0.981	0.964	0.969
Dubinin–Radushkevich (D–R)			
Q_D	1.90	2.57	2.22
K	1×10^{-5}	4×10^{-6}	9×10^{-6}
E_s	0.223	0.353	0.235
R^2	0.784	0.823	0.820
Temkin			
A	0.4129	1.0281	0.5704
B	0.51	0.577	0.554
b	4.776	4.365	4.472
R^2	0.977	0.987	0.984

consideration.

Langmuir isotherm

The adsorption capacity of the adsorbent is considered one of the important parameters for design purpose. The linearized Langmuir isotherm equation (Equation 1) was used to obtain the maximum monolayer adsorption capacity of RB adsorption onto MLP surface (Langmuir, 1918).

$$C_e/q_e = 1 / bQ_m + (1/Q_m)C_e \quad (1)$$

where, b is adsorption equilibrium constant (L/mg) that is related to the apparent energy of adsorption and Q_m is the quantity of adsorbate required to form a single monolayer on unit mass of adsorbent (mg/g) and q_e is the amount adsorbed on unit mass of the adsorbent (mg/g) when the equilibrium concentration is C_e (mg/L).

The isotherm plots of *Ce/qe* vs. *Ce* for the adsorption of RB onto MLP is shown in Figure 8. The Langmuir constants Q_m, and b, evaluated from the slope and intercepts of these plots, along with the correlation coefficients are summarized in Table 1.

The high R^2 values (0.988-0.995) indicate that

Table 2. Adsorption capacities of Rhodamine B on various adsorbents.

Adsorbent	Maximum adsorbent capacity, Q_m (mg/g)	References
Fly ash	2.33	Khan et al. (2009)
Iron chromium oxide (ICO)	2.98	Kannan and Murugavel (2007)
Tamarind fruit shells activated carbon	3.94	Vasu (2008)
Coir pith	2.56	Namasivayam et al. (2001)
Coal	1.24	Khan et al. (2004)
Raw orange peel	3.23	Namasivayam et al. (1996)
Mango leaf powder (MLP)	3.31	Present study

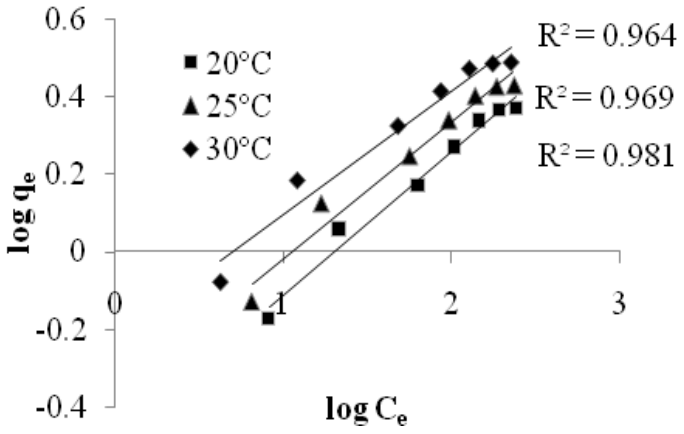

Figure 9. Freundlich Isotherm plot.

adsorption follows Langmuir model, with Q_m = 3.31 mg/g and b = 5.51 L/mg at 30°C. The higher value of Q_m (>> 1) indicates a strong adsorbate-adsorbent interaction. A comparison of adsorbent capacity of MLP with many low cost adsorbents (Table 2) indicates that MLP has a greater adsorption capacity than fly ash, iron chromium oxide, coir pith coal and raw orange peel.

The separation factor ($R_L = 1/1 + bC_e$), which is a measure of adsorption favorability (Hall et al., 1966) was evaluated with a view to predict whether the adsorption is favorable. The R_L values (Table 1) are in between 0 and 1, thus validating a favorable adsorption process. The Langmuir constant, Q_m increased with increasing temperature, which suggested that adsorption of RB onto MLP is endothermic.

Freundlich isotherm

The Freundlich isotherm considers multilayer adsorption with a heterogeneous energetic distribution of active sites, accompanied by interactions between adsorbed molecules (Freundlich, 1906). The linear Freundlich isotherm is expressed as:

$$\log q_e = \log K_f + 1/n \log C_e \quad (2)$$

where, K_f [(mg/g)/(mg)$^{1/n}$] is the Freundlich constant, which indicates the relative adsorption capacity of the adsorbent, and n is a measure of the adsorption intensity or surface heterogeneity (a value closer to zero represents a more heterogeneous surface).

The linear plots of $log\ K_f$ versus $log\ C_e$ (Figure 9) shows that the adsorption of RB onto MLP also follows Freundlich isotherm model. The Freundlich constants (K_f and n) and correlation coefficients are recorded in Table 1. The value of n (2.72-3.12) indicates favorable adsorption. As evident from the regression correlation coefficients (Table 1), the Langmuir model gives a better fit (R^2=0.995) than the Freundlich model (R^2 = 0.964).

Dubinin–Radushkevich (D–R) isotherm

The linear form of D-R equation (Equation 3) (Dubinin and Radushkevich, 1947) was used to evaluate the porosity and apparent adsorption energy:

$$ln q_e = ln Q_D - K\varepsilon^2 \quad (3)$$

where K (mol^2 /kJ^2) is a constant related to the adsorption energy; Q_D (mg/g) is the maximum D-R adsorption capacity; and ε (Polyani potential) can be calculated from

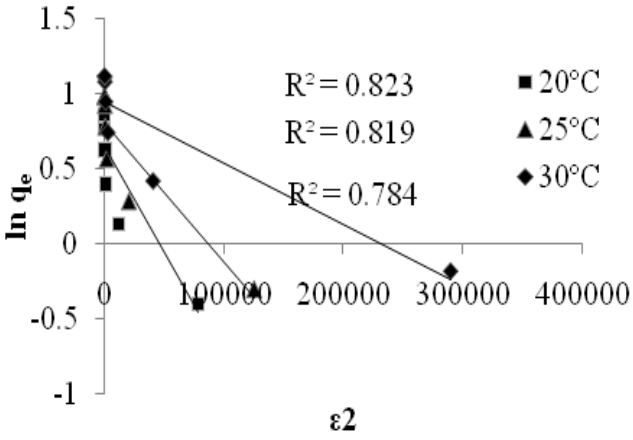

Figure 10. Dubinin–Radushkevich (D–R) isotherm plot.

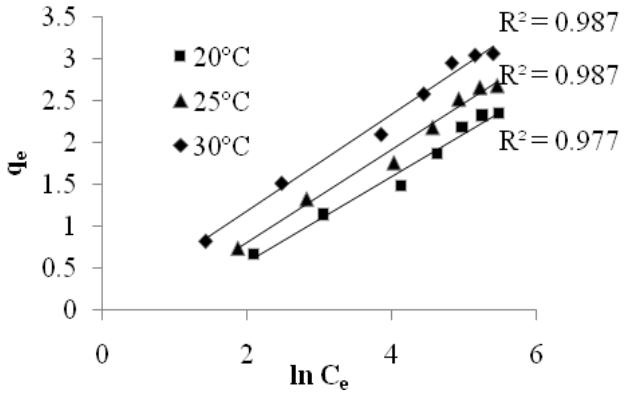

Figure 11. Temkin isotherm plot.

Equation 4:

$$\varepsilon = RTln(1 + 1/C_e) \quad (4)$$

The adsorption energy, E_s was calculated using Equation 5:

$$E_s = 1 / (2\beta)^{1/2} \quad (5)$$

The D-R isotherm constants, K and Q_D, calculated from the slope and intercept of the plot between ln q_e and ε^2 (Figure 10), are recorded in Table 1. The values of porosity factor (K) less than unity (4×10^{-6} mol^2/kJ^2) indicated a micro-porous MLP surface, and the surface heterogeneity may be attributed to the pore structure as well as sorbate-adsorbent interaction (Kim et al., 1995). The maximum adsorption capacity, Q_D, obtained from D-R model (2.57 mg/g) for adsorption of dye by MLP is less than Langmuir adsorption capacity (Q_m = 3.11 mg/g). The poor correlation coefficient (R^2 = 0.784-0.823) indicates that the D-R isotherm model did not satisfactorily fit the adsorption data.

Temkin isotherm

The linear form of Temkin isotherm model is given by the following Equation (6) (Temkin and Pyzhev, 1940):

$$q_e = B\ln A + B\ln C_e \quad (6)$$

where B (=RT/b) is a constant representing the heat of adsorption b (KJ/mol) and A is the equilibrium binding constant (L/mg) corresponding to maximum binding energy.

A plot of q_e versus $ln\ C_e$ (Figure 11) gives a straight line, with slope representing B and intercept equal to K. The Temkin constants along with the correlation coefficients are tabulated in Table 1. The R^2 values (0.987-0.977) confirm that Temkin isotherm provides a reasonable model for the adsorption of RB onto MLP. However, from the comparison of the adsorption

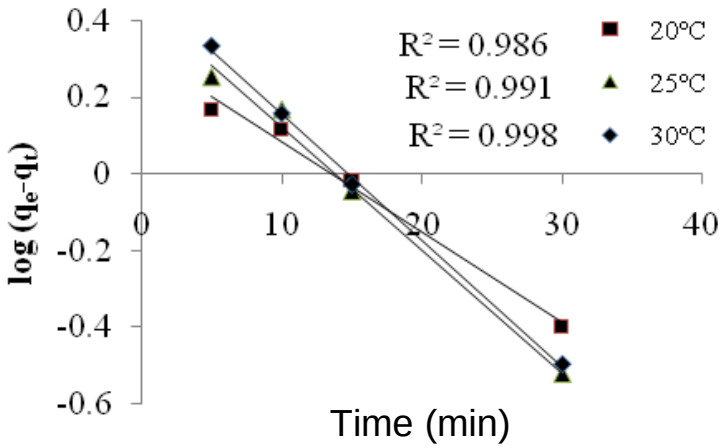

Figure 12. Lagergren pseudo-first order kinetic plot.

Table 3. Kinetic parameters for the adsorption of RB onto MLP.

Kinetic model	20°C	25°C	30°C
q_e (mgg^{-1}) Experimental	2.2	2.62	3.04
Lagergren pseudo-first order			
q_e Calculated	2.07	2.76	3.08
K_{ad}	0.053	0.074	0.076
R^2	0.986	0.991	0.998
Pseudo-second order			
q_e Calculated	3.01	3.47	3.92
K_2	0.0169	0.0174	0.0175
h	0.153	0.210	0.269
R^2	0.980	0.988	0.991
Elovich			
α	0.3189	0.4047	0.5030
β	1.4534	1.1668	1.009
R^2	0.953	0.980	0.995
Intra particle diffusion			
K_{ip}	0.34	0.414	0.47
C_{ip}	-0.087	-0.050	0.049
R^2	0.991	0.972	0.952
Film diffusion			
K_{fd}	0.053	0.073	0.076
R^2	0.986	0.991	0.998

isotherms it can be seen that best adsorption was described by Langmuir model followed by Temkin and Freundlich isotherm models.

Adsorption dynamics

The adsorption kinetics is a useful parameter in the design of industrial adsorption columns. The rate constants for adsorption of RB onto MLP were evaluated using pseudo-first order and pseudo-second order kinetic models.

The linear form of pseudo-first order kinetic model is given by Equation 7 (Lagergren, 1898):

$$\log (q_e - q_t) = \log(q_e) - K_{ad}/2.303\, t \quad (7)$$

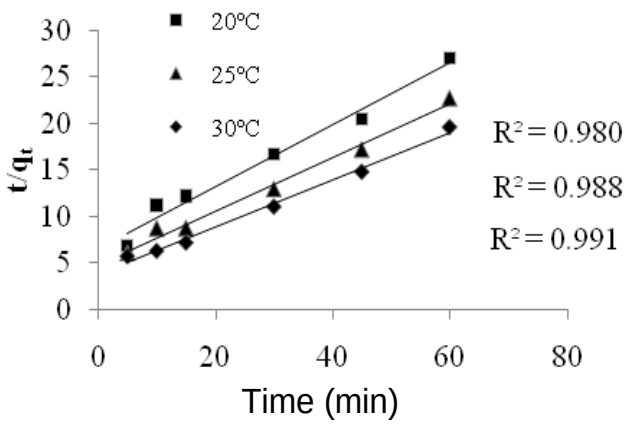

Figure 13. Pseudo-second order kinetic plot.

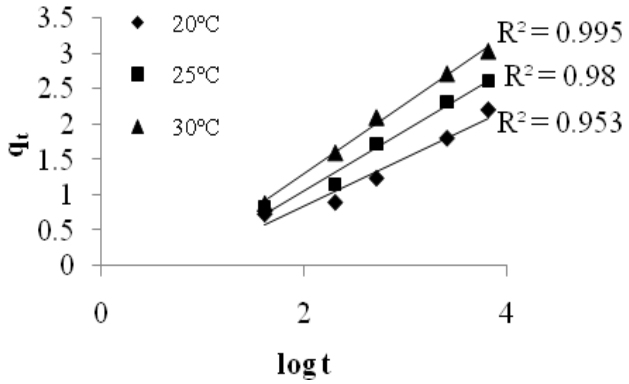

Figure 14. Elovich plot for RB adsorption onto MLP.

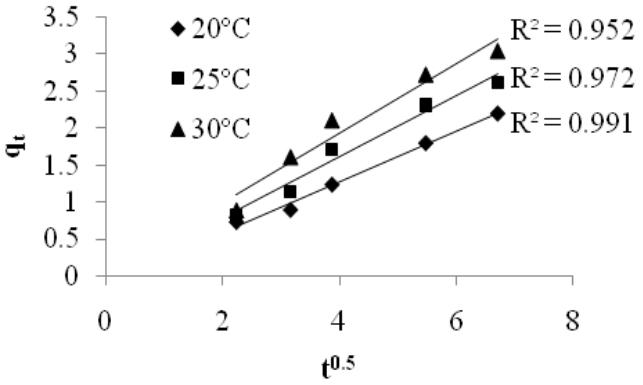

Figure 15. Intraparticle diffusion plot.

where, q_e and q_t are the amounts of RB sorbed (mg/g) at equilibrium and at any time, t respectively, and k_1 (l/min) is the pseudo-first order rate constant.

The adsorption rate constant, k_1 and q_e has been computed from the straight plot of log ($q_e - q_t$) vs. t (Figure 12), and are listed in Table 3. The pseudo-second order kinetic model is given by Equation 8 (Ho and Mckay, 1998, 1999):

$$t/q_t = 1/k_2 q_e^2 + (1/q_e)t \quad (8)$$

where, k_2 (g/mg/min) is the pseudo-second order rate constant.

The plot of t/qt *vs.* t is shown in Figure 13. The values of q_e, k_2 and correlation coefficients are reported in Table 3. The regression correlation coefficients (0.986-0.998) and a good agreement between the calculated and experimental q_e values for pseudo-first order model indicated that the adsorption of dye onto MLP is governed by pseudo-first order rate kinetics.

Elovich model

The linear form of Elovich equation (Chien and Clayton, 1980) is expressed as follows (Equation 9):

$$qt = 1/\beta \ln(\alpha\beta) + 1/\beta \ln t \quad (9)$$

where, α (mg/g/min) is the initial adsorption rate and β (g/mg) is the desorption constant related to the extent of the surface coverage and activation energy for chemisorption. The values of kinetic constants α and β were calculated (Figure 14) and listed in Table 3. It is found that adsorption and desorption rate increased and decreased with temperature respectively. The regression correlation coefficients (R^2) are obtained in the range of 0.953-0.995.

Intraparticle diffusion model

The experimental data was analyzed using intraparticle diffusion model with a view to elucidate the diffusion mechanism (Weber and Morris, 1963). The intraparticle diffusion rate constant, K_{ip} (mg/g $min^{0.5}$) can be obtained from the slope of the plot of q_t (mg/g) versus $t^{0.5}$ according to the following equation:

$$K_{ip} = Q_t/t^{0.5} + C_{ip} \quad (10)$$

where C_{ip} (mg/g) is a constant, which gives idea about the thickness of the boundary layer and can be calculated from the intercept of the plot. The larger the C_{ip}, greater is the contribution of surface adsorption in the rate limiting step.

According to this model, a linear plot of q_t versus $t^{0.5}$ indicated that the uptake process was controlled by intraparticle diffusion. On the other hand, plot showed multi-linearity; indicating adsorption process as controlled by two or more steps. In the present study, the plot of q_t *versus* $t^{0.5}$ gives a straight line (Figure 15), which passes from the origin, indicating that the adsorption process

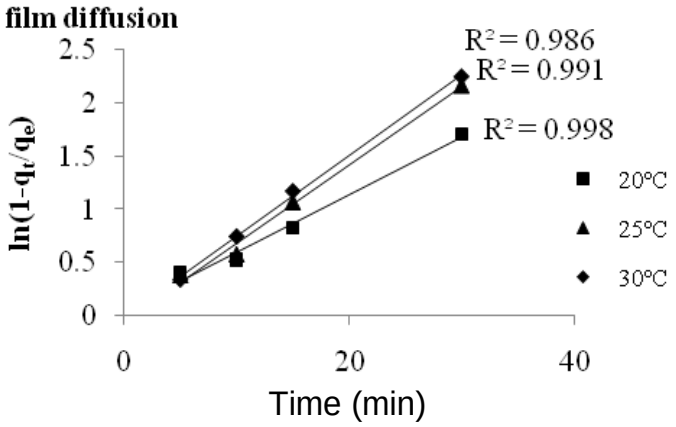

Figure 16. Film diffusion plot.

tends to be intraparticle diffusion controlled. The values of K_{ip} and C_{ip} along with the regression correlation coefficients are listed in Table 3.

Film diffusion model

During the transport of the RB molecules from the liquid phase up to the solid phase, the boundary plays a significant role in adsorption; the liquid film diffusion model may be applied as follows (Equation 11):

$$\ln(1 - q_t/q_e) = -K_{fd}.t \quad (11)$$

where q_t/q_e (= F) is the fractional attainment of equilibrium, and K_{fd} is the film diffusion rate constant. A linear plot of *–ln (1-F) vs. t* with zero intercept would suggest that the kinetics of the adsorption process is diffusion controlled. The plot of $1/(1-q_t/q_e)$ *vs. t* gives a straight line (Figure 16), with slope equal to K_{fd} and suggested that adsorption of RB is controlled by diffusion through the liquid film surrounding the solid adsorbent. The values of K_{fd} and the regression correlation coefficients are listed in Table 3.

Thermodynamic parameters

In order to confirm the feasibility and the nature of adsorption process, thermodynamic parameters were calculated using the following equations at different temperature (20 to 30°C):

$$\Delta G^{\circ} = -RT\ln b' \quad (12)$$

$$\Delta H^{0} = -R\left(\frac{T_2T_1}{T_2 - T_1}\right)\ln\frac{b_2}{b_1} \quad (13)$$

$$\Delta S^{\circ} = \frac{\Delta H^{\circ} - \Delta G^{\circ}}{T} \quad (14)$$

$$E_a = \Delta H^{\circ} + RT \quad (15)$$

where b', b_2, and b_1 are the Langmuir constants at 20, 25 and 30°C, respectively. The other terms have their usual meanings. The thermodynamic data for the adsorption of RB onto MLP are summarized in Table 4.

The negative values of ΔG° indicate the spontaneity of the uptake process while the positive values of ΔH° imply that adsorption phenomenon is endothermic. The positive values of ΔS° suggest favorable affinity of the adsorbent for the dyes.

Conclusions

The equilibrium, kinetics and thermodynamics for the uptake of Rhodamine B dye by MLP from aqueous solution were studied. The adsorption data was fitted the best in Langmuir adsorption model. The kinetics data agreed well with pseudo-first order rate equation. The fitness of Langmuir's model indicated the formation of monolayer coverage of the sorbate on the outer surface of the adsorbent. The negative values of ΔG° and positive values of ΔH° and ΔS° indicated adsorption process as spontaneous, endothermic and favorable. Besides, the results indicated that the MLP adsorbent is capable for the removal of RB with high affinity and capacity indicating its potential use as a low cost adsorbent in near future.

REFERENCES

Ali I (2010). The Quest for Active Carbon Adsorbent Substitutes: Inexpensive Adsorbents for Toxic Metal Ions Removal from Wastewater. Sep. Purif. Revp, 39: 95-171.

Allen SJ, Koumanova B. (2005). Discolourization of water/wastewater using adsorption (review). J. Univ. Chem. Technol. Metallur., 40: 175-192.

Amin NK (2008). Removal of reactive dye from aqueous solutions by adsorption onto activated carbons prepared from sugarcane baggasse pith. Desalination, 223: 152-161.

Arivoli S, Thenkuzhali M (2008). Kinetic, mechanistic, thermodynamic and equilibrium studies on the adsorption of Rhodamine B by acid activated low cost carbon. E-J. Chem., 5(2): 187-200.

Arivoli S, Thenkuzhalib M, Prasath PMD (2009). Adsorption of rhodamine B by acid activated carbon-kinetic, thermodynamic and equilibrium studies. Orbital, 1: 138-155.

Chien SH, Clayton WR (1980). Application of Elovich equation to the kinetics of phosphate release and adsorption on Soils. Soil Sci. Soc. Am. J., 44: 265-268.

Crini G (2006). Non-conventional low-cost adsorbents for dye removal: A review. Bioresour. Technol., 97(9): 1061-1085.

Dubinin MM, Radushkevich LV (1947). Equation of the characteristic curve of activated charcoal. Chem. Zentr., 1: 875.

Freundlich H (1906). Concerning adsorption in solutions. J. Phys. Chem.-Stochiometrie Verwandtschaftslehre, 57A: 385–470.

Gupta VK, Ali I, Saini VK, Gerven TV, Van der Bruggen B, Vandecasteele C (2005). Removal of dyes from wastewater using

bottom ash. J. Ind. Eng. Chem. Res., 44: 3655-3664.
Gupta VK, Ali I, Suhas, Mohan D (2003). Equilibrium uptake sorption for the removal of a basic dye (basic red) using low cost adsorbent. J. Colloid Interf. Sci., 265: 257-264.
Hall KR, Eagleton LC, Acrivos A, Vermeulen T (1966). Pore and solid diffusion kinetics in fixed bed adsorption under constant pattern conditions. Ind. Eng. Chem. Fundam., 5: 212–219.
Hema M, Arivoli S (2007). Comparative study on the adsorption kinetics and thermodynamics of dyes onto acid activated low cost carbon. Int. J. Phys. Sci., 2(1): 10-17.
Hema M, Arivoli S (2009). Rhodamine B adsorption by activated carbon: Kinetic and equilibrium studies. Indian J. Chem. Technol., 16: 38-45.
Ho YS, Mckay G (1998). Kinetic model for lead(II) adsorption on to peat. Adsorption Sci. Technol., 16: 243-255.
Ho YS, McKay G (1999). Pseudo second order model for adsorption processes. Process Biochem., 34: 451–465.
Inbaraj BS, Sulochana N (2006). Use of jackfruit peel carbon (JPC) for adsorption of rhodamine-B, a basic dye from aqueous solution. Indian J. Chem. Technol., 13: 17-23.
Kannan N, Murugavel S (2007). Column studies on the removal of dyes Rhodamine-B, congo red and acid violet by adsorption on various adsorbents. EJEAFChem., 6: 1860-1868.
Khan TA, Ali I, Singh VV, Sharma S (2009). Utilization of fly ash as low-cost adsorbent for the removal of methylene blue, malachite green and rhodamine B dyes from textile wastewater. J. Environ. Protect Sci., 3: 11-22.
Khan TA, Singh V, Kumar D (2004). Removal of some basic dyes from artificial textile wastewater by adsorption on Akash kinari coal. J. Sci. Ind. Res., 63: 355-364.
Kim BT, Lee HK, Moon H, Lee KJ (1995). Adsorption of radionuclides from aqueous solutions by inorganic adsorbents. Sep. Purif. Technol., 30: 3165-3182.
Lagergren S (1898). About the theory of so-called adsorption of solute substances. Kungliga Svenska Vetenskapsakademiens, 24: 1-39.
Langmuir I (1918). The adsorption of gases on plane surfaces of glass, mica and platinum. J. Am. Chem. Soc., 40: 1361–1367.
Low KS, Lee CK, Tan KK (1995). Biosorption of basic dyes by water hyacinth roots. Bioresour. Technol., 52: 79-83.
Mondal S (2008). Methods of dye removal from dye house effluents–An overview. Environ. Eng. Sci., 25: 383-396.
Namasivayam C, Muniasamy N, Gayathri K, Rani M, Ranganathan K (1996). Removal of dyes from aqueous solutions by cellulose waste orange peel. Bioresour. Technol., 57: 37-43.
Namasivayam C, Radhika R, Suba S (2001). Uptake of dyes by a promising locally available agricultural solid waste: Coir pith. Waste Manage., 21(4): 381-387.
Poots VJP, Mckay G, Healy JJ (1976). The removal of acid dye from effluent using natural adsorbents-I. Peat, Water Res., 10: 1067-1070.
Preethi S, Sivasamy A, Sivanesan S, Ramamurthi V, Swaminathan G (2006). Removal of safranin basic dye from aqueous solutions by adsorption onto corncob activated carbon. Ind. Eng. Chem. Res., 45: 7627-7632.
Rajamohan N (2009). Equilibrium studies on adsorption of an anionic dye onto acid activated water hyacinth roots. Afr. J. Environ. Sci. Technol., 3: 399-404.
Ramuthai S, Nandhakumar V, Thiruchelvi M, Arivoli S, Vijayakumaran V (2009). Rhodamine B adsorption-kinetic, mechanistic and thermodynamic studies. E-J. Chem., 6(S1): S363-S373.
Sivaraj R, Sivakumar S, Senthilkumar P, Subburam V (2001). Carbon from cassava peel, an agricultural waste, as an adsorbent in the removal of dyes and metal ions from the aqueous solution. Bioresour. Technol., 80: 233-235.
Tan IAW, Hameed BH, Ahmad AL (2007). Equilibrium and kinetic studies on basic dye adsorption by oil palm fibre activated carbon. Chem. Eng. J., 127: 111-119.
Temkin MJ, Pyzhev V (1940). Recent modifications to Langmuir isotherms, Acta Physiochem. USSR, 12: 217-222.
Vasu AE (2008). Studies on the removal of rhodamine b and malachite green from aqueous solutions by Tamarind fruit shells activated carbon. E-J Chem., 5(4): 844-852.
Weber WJ, Morris JC (1963). Kinetics of adadsorption on carbon from solution. J. Sanit. Eng. Div. Am. Soc. Civ. Eng., 89: 31-60.